Journal of the Chinese Society of Mechanical Engineers, Vol.46, No.6, pp591~599 (2025)

Structural Analysis of Natural Fiber Reinforced Composites in Bicycle Frames

Chi-Hua Hsu* and Yan-Cheng Chen**

Keywords：natural Fiber Reinforced Composites, bicycle frames, finite element method.

ABSTRACT

In response to the growing demand for sustainable and lightweight bicycle structures, this study investigates the application of natural fiber-reinforced composites in frame design. Sisal and jute fibers were selected as reinforcement materials, and their mechanical performance was evaluated through finite element simulations based on the ISO 4210-6 impact test standard. A composite stacking block consisting of four fiber orientations (0°, 30°, 60°, and 90°) was used to assess the minimum laminate thickness required for impact compliance. Results revealed that the sisal composite exhibited higher stiffness than jute. Furthermore, local reinforcement strategies were explored by applying targeted lay-ups to high-deformation regions (top tube and down tube). The findings showed that localized ply additions effectively reduced deformation while minimizing material usage, with the top tube exhibiting greater reinforcement efficiency. These results confirm the potential of natural fiber composites as viable, eco-friendly alternatives for bicycle frame applications.

INTRODUCTION

With the increasing global emphasis on sustainability and environmental protection, bicycles have emerged not only as traditional means of transportation but also as prominent solutions for urban commuting and recreational activities. To meet the demand for lightweight and high-performance structures, frame materials have evolved from conventional metals to advanced composites such as carbon and glass fiber. However, these synthetic fibers involve energy-intensive manufacturing processes, are non-biodegradable, and impose significant environmental burdens, making them less aligned with the goals of sustainable design.

Natural fiber-reinforced composites (NFRCs) have garnered attention as viable alternatives due to their low density, renewability, biodegradability, and satisfactory mechanical properties. Khan et al. (2024) highlighted that surface-treated natural fibers can significantly enhance interfacial bonding and improve mechanical performance. Nurazzi (2021) emphasized hybrid fiber strategies to overcome the brittleness and fatigue limitations of single-fiber systems. Karimah (2021) and Khalid (2021) addressed challenges in fiber–matrix compatibility and moisture absorption, which can be mitigated through chemical modifications such as alkali and silane treatments. In structural applications, Chaikittiratana (2019) applied traditional hemp fibers to bicycle frame components using filament winding and finite element analysis (FEA), demonstrating their potential as replacements for steel tubes. Saravanan (2021) compared various natural fibers for automotive structural panels and found that jute and sisal offered excellent structural stability. Rahman (2021) evaluated flax composites for sports equipment, citing their superior damping and strength-to-weight ratio for dynamic structures. From a simulation perspective, Naveen and Reddy (2018) utilized ANSYS Composite PrepPost (ACP) to model ply sequences and conduct static structural analyses, validating the efficiency of composite materials for load-bearing shafts. Lin et al. (2017) further demonstrated that sensitivity analysis integrated with FEA is effective in optimizing design parameters and improving frame stiffness. While extensive studies have explored NFRCs in various engineering fields, systematic evaluations of their use in bicycle frame structures remain limited, particularly concerning the effects of ply orientation and stacking sequences on mechanical performance.

This study utilizes jute and sisal fibers, reinforced with epoxy resin, to construct laminated composite models for structural evaluation. A falling

Paper Received July, 2025. Revised September, 2025. Accepted October, 2025. Author for Correspondence: Chi-Hua Hsu

* *Assistant Professor, Department of Mechatronics Engineering, National Changhua University of Education, Changhua, Taiwan 500208, ROC.*

** *Graduate Student, Department of Mechatronics Engineering, National Changhua University of Education, Changhua, Taiwan 500208, ROC.*

mass impact test is simulated in accordance with ISO 4210-6 standards using the ANSYS finite element analysis platform. The analysis focuses on assessing the influence of ply orientation on structural integrity, with the aim of identifying optimized stacking configurations that enhance mechanical performance. The findings are intended to serve as a technical foundation and design reference for the sustainable integration of natural fiber-reinforced composites in bicycle frame applications.

Fundamental Theories of Composite Materials

Composite materials consist of a matrix and reinforcement phase, where the matrix maintains structural form and transfers loads, while fibers provide mechanical strength. Matrices may be polymers, metals, or ceramics, and fibers can be synthetic (e.g., carbon, glass) or natural (e.g., jute, sisal). Combined, these materials form anisotropic systems with enhanced properties. The basic unit, a lamina, features fibers aligned in specific directions. Laminates are formed by stacking multiple laminae with varied orientations (e.g., 0°, ±45°, 90°) to achieve multidirectional strength, as show in Figure 1. To resist complex loads, layups must optimize stress distribution and deformation behavior. Symmetric and balanced stacking further reduces coupling effects and thermal stresses, improving overall structural performance.

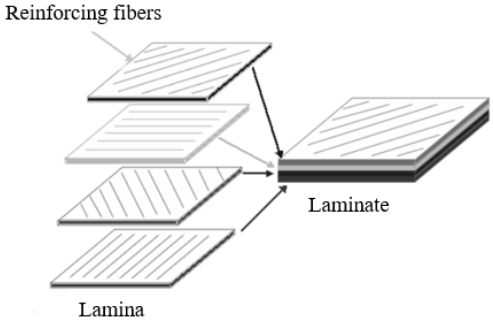

Figure 1. Schematic diagram of a laminate (modified from Fao, 2016)

Stress–Strain Relationship of a Lamina

In composite mechanics, a lamina is the fundamental structural unit composed of fibers embedded within a matrix, exhibiting highly anisotropic behavior. To describe its mechanical response under in-plane loading, the lamina is typically modeled as a thin, orthotropic layer, where the fiber direction is defined as the 1-axis (longitudinal), the transverse direction as the 2-axis, and the thickness direction as the 3-axis. According to Classical Lamination Theory (CLT), the in-plane stress–strain relationship of a lamina can be expressed as:

$$\begin{Bmatrix} \varepsilon_1 \\ \varepsilon_2 \\ \gamma_{12} \end{Bmatrix} = \begin{bmatrix} Q_{11} & Q_{12} & Q_{16} \\ Q_{12} & Q_{22} & Q_{26} \\ Q_{16} & Q_{26} & Q_{66} \end{bmatrix}^{-1} \begin{Bmatrix} \sigma_1 \\ \sigma_2 \\ \tau_{12} \end{Bmatrix} \quad (1)$$

where σ1, σ2, τ12 represent the normal and shear stresses in the principal material directions, while ε1, ε2, γ12 are the corresponding strain components. The stiffness matrix [Q] is determined by the lamina's elastic properties, including the fiber and matrix Young's moduli, shear modulus, and Poisson's ratios. When the fiber orientation does not align with the global loading direction, the stiffness matrix must be transformed to an off-axis orientation θ. The transformed stiffness matrix [Q′] is calculated using:

$$\left[Q^{'}\right] = [T]^{-1}[Q][T]^{-T} \quad (2)$$

This transformation allows evaluation of the mechanical behavior of a lamina at arbitrary fiber angles.

Constitutive Relations of a Laminate

A laminate is formed by stacking multiple laminae with varying fiber orientations. Its overall mechanical behavior depends on ply properties, thicknesses, and stacking sequence. Based on Classical Lamination Theory, the relationship between in-plane forces/moments and mid-plane strains/curvatures is expressed as:

$$\begin{bmatrix} N \\ M \end{bmatrix} = \begin{bmatrix} A & B \\ B & D \end{bmatrix} \begin{Bmatrix} \varepsilon^0 \\ \kappa \end{Bmatrix} \quad (3)$$

Where ε^0 represents mid-plane strains, and κ denotes curvatures. Matrices A, B, and D represent the extensional, coupling, and bending stiffness matrices, respectively. Symmetric laminates have B=0, decoupling stretching and bending responses. Proper stacking design allows engineers to tailor stiffness and strength characteristics to meet performance requirements in composite structures.

Rule of Mixtures for Composite Materials

The Rule of Mixtures is a commonly used theoretical model for estimating the effective mechanical properties of composite materials during the preliminary design stage. Assuming uniform fiber distribution and perfect bonding at the fiber–matrix interface, this model provides closed-form expressions for predicting the longitudinal and transverse elastic moduli of laminated composites, given by:

$$E_L = V_f E_f + V_m E_m, \quad \frac{1}{E_T} = \frac{V_f}{E_f} + \frac{V_m}{E_m} \tag{4}$$

where E_L and E_T are the longitudinal and transverse moduli, V_f and V_m are the volume fractions, and E_f, E_m denote the moduli of the fiber and matrix, respectively. In this study, the Rule of Mixtures is applied to estimate the effective elastic properties of natural fiber-reinforced laminates. These properties serve as the input parameters for the finite element analysis (FEA) model.

Tsai-Wu Failure Criterion

In composite structural analysis, failure prediction is essential for both simulation accuracy and design reliability. The Tsai-Wu failure criterion is widely used for anisotropic materials, as it accounts for differences in tensile and compressive strengths, as well as the interaction effects between stress components. The Tsai-Wu failure equation is given by:

$$F_1\sigma_1 + F_2\sigma_2 + F_{11}\sigma_1^2 + F_{22}\sigma_2^2 + F_{66}\tau_{12}^2 + 2F_{12}\sigma_1\sigma_2 \le 1 \tag{5}$$

where σ_1 and σ_2 are the normal stresses in the material principal directions, and τ_{12} is the in-plane shear stress. The strength coefficients are defined as:

$$F_1 = \frac{1}{X_T} - \frac{1}{X_C}, \quad F_2 = \frac{1}{Y_T} - \frac{1}{Y_C}, \quad F_{11} = \frac{1}{X_T} - \frac{1}{X_C}$$

$$F_{22} = \frac{1}{Y_T} - \frac{1}{Y_C}, \quad F_{66} = \frac{1}{S^2}, \quad F_{12} = -\frac{1}{2}\sqrt{F_{11}F_{12}}$$

Where X_T and X_C are the longitudinal tensile and compressive strengths; Y_T and Y_C are the transverse tensile and compressive strengths, and S is the in-plane shear strength. A value of 1 indicates the onset of failure, while values exceeding 1 represent material failure under the given stress state. In finite element simulations, the Tsai-Wu criterion is frequently employed to evaluate failure initiation at the element level. This allows for the identification of critical regions and informs ply optimization strategies aimed at enhancing structural reliability and performance.

Finite Element Modeling of the Bicycle Frame

This section utilizes the finite element method, implemented via the ANSYS Workbench platform, to simulate the structural behavior of a bicycle frame made from natural fiber-reinforced composites. The analysis focuses on the frame's response under falling mass impact, conducted in accordance with ISO 4210-6 standards, with the aim of providing practical insights for future ply design and material application.

Geometric Modeling and Composite Material Parameter Definition

The 3D assembly model of the bicycle frame, front fork, and dropouts was constructed using SolidWorks, as shown in Fig. 2. To focus the analysis on the effects of ply configurations of natural fiber-reinforced composites on the structural behavior of the frame, the mechanical responses of the front fork and dropouts was excluded from the simulation. These components were retained solely to serve as geometric references for boundary conditions and load transfer.

For material definition, the bicycle frame was assigned as a natural fiber-reinforced composite, incorporating sisal and jute fibers as reinforcements and epoxy resin as the matrix. The effective material properties of the composites were estimated using the rule of mixtures from Eq. (4), assuming a 50:50 volume fraction between fibers and matrix, with a single lamina thickness of 0.2 mm. The resulting material parameters for the sisal and jute composites are listed in Table 1 and 2, respectively.

Table 1. Material Properties of Sisal Fiber-Reinforced Composite

Young's Modulus (MPa)		
E1	*E2*	*E3*
36500	*3396*	*3396*
Poisson's Ratio		
V12	*V13*	*V23*
0.375	0.0349	0.375
Shear modulus (MPa)		
G12	G13	G23
1912	1338	1912
Tensile strength (MPa)		
XT	YT	ZT
249.5	21	21
Compressive strength (MPa)		
XC	YC	ZC
174.7	42	42
Shear strength (MPa)		
S12	S13	S23
20	14	20

Table 2. Material Properties of Jute Fiber-Reinforced Composite

Young's Modulus (MPa)		
E1	*E2*	*E3*
36500	*2915*	*2915*
Poisson's Ratio		
V12	*V13*	*V23*
0.35	0.0346	0.35
Shear modulus (MPa)		
G12	G13	G23
1837	1285.9	1837
Tensile strength (MPa)		
XT	YT	ZT
110.5	21	21
Compressive strength (MPa)		
XC	YC	ZC
77.35	42	42
Shear strength (MPa)		
S12	S13	S23
20	14	20

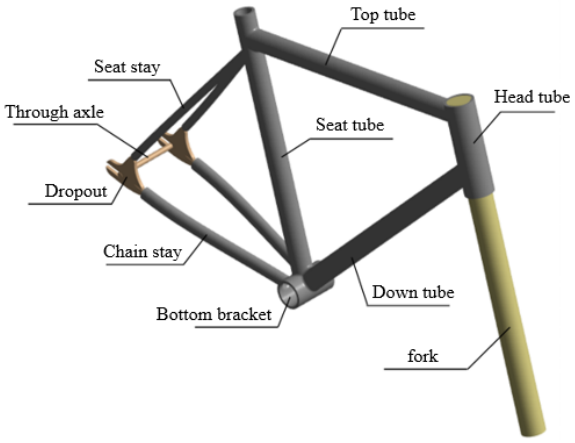

Figure 2. Bicycle Frame Structure Diagram

Composite Laminate Modeling and Simulation Setup

Following the completion of geometric modeling and material parameter definition, composite laminate modeling and simulation setup were performed using the ACP (ANSYS Composite PrepPost) module within the ANSYS Workbench environment. ACP is a specialized simulation environment tailored for laminated composite structures, enabling the definition of anisotropic material properties, control of ply orientations, and assignment of region-specific layup configurations. The module also integrates seamlessly with structural solvers for evaluating mechanical behavior and potential failure under various loading conditions.

The ACP modeling process consists of six key configuration steps:

1. Fabric Properties – Define the material properties of the fiber and matrix materials.
2. Stackup Properties – Specify the ply angles, thicknesses, and stacking sequence.
3. Rosette Properties – Create local coordinate systems to reference ply directions.
4. Oriented Selection Set – Associate orientation data with selected geometric regions.
5. Modeling Ply Properties – Apply ply definitions to the 3D model geometry.
6. Solid Model Properties – Convert the laminate model into a solid body suitable for finite element analysis.

ISO 4210-6 Bicycle Frame Impact Test Modeling

This study adopts the ISO 4210-6 bicycle testing standard, established by the International Organization for Standardization (ISO), as the basis for structural simulation of natural fiber-reinforced composites applied to bicycle frame design. Figure 3 illustrates the drop impact test defined in the ISO 4210-6 standard. According to the test configuration, a through axle must be mounted vertically onto the fixture (position No. 5) and allowed to rotate freely, replicating realistic boundary conditions. And then, a 22.5 kg drop mass is suspended above the front fork and released from a specified height h1, as indicated in Table 3, to apply a vertical impact to the fork. According to the ISO 4210-6 standard, the permanent deformation of the front fork after impact must not exceed 10 mm to satisfy the regulatory safety requirement.

Table 3. Component Definitions and Labels in ISO 4210-6 Impact Test Setup

Key	
1	wheelbase
2	permanent deformation
3	22.5 kg striker
4	low-mass roller (1 kg max.)
5	rigid mounting for rear-axle attachment point
6	direction of rearward impact
h_1	drop heigh

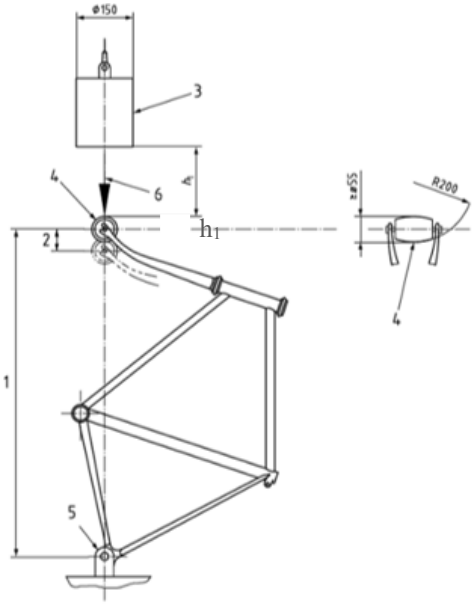

Figure 3. Impact test of ISO 4210-6

To implement the impact test in the finite element model, all relevant boundary and loading conditions were consolidated and illustrated in Figure 4. This figure presents the complete boundary setup applied to the bicycle frame, with labeled regions A through D denoting specific boundary conditions. Region A denotes the location where an 826 N force was applied in the negative X-direction at the front fork, simulating the vertical impact from a 22.5 kg drop mass. Region B illustrates the cylindrical support located at the through-axle (position No. 5), which permits free rotation along the tangential direction. Region C denotes the remote displacement conditions at the dropout, where all translational degrees of freedom were fixed and only the Z-axis rotation was left unconstrained. Lastly, Region D marks the bottom support of the frame, where translation in the X and Y directions was allowed while displacement along the Z-axis was restricted to emulate ground contact. These settings ensure that the simulation closely approximates the physical conditions defined in the ISO 4210-6 standard.

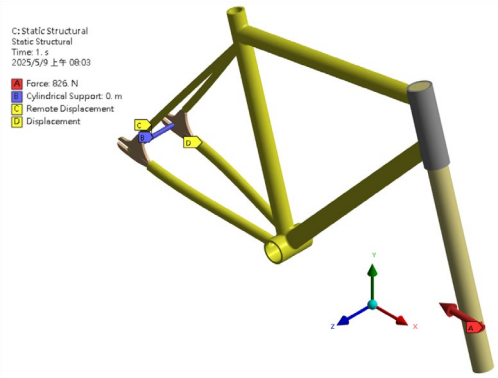

Figure 4. Boundary Condition Setup for Bicycle Frame Drop Impact Test

RESULTS AND DISCUSSIONS

This study investigates the feasibility of applying natural fiber-reinforced composites to bicycle frame structures by conducting impact test simulations in accordance with the ISO 4210-6 international testing standard. Jute and sisal fibers were selected as the reinforcing materials, and their structural performance was evaluated under varying ply orientations and stacking sequences. To further explore lightweight design strategies without compromising mechanical integrity, local reinforcement was applied to specific regions of the frame to enhance overall structural performance.

Mesh Convergence Analysis

Since the finite element method (FEM) discretizes the problem domain into a finite number of mesh elements for numerical computation, the accuracy of its numerical solutions is closely related to the mesh density. To ensure the reliability and stability of the simulation results, a mesh convergence analysis was first conducted and used as the basis for subsequent modeling procedures. Five different mesh sizes (1.8 mm, 1.5 mm, 1.2 mm, 1.0 mm, and 0.8 mm) were evaluated to verify numerical accuracy. The corresponding number of elements ranged from 727,964 to 2,578,184. As shown in Figure 5, the deformation results gradually stabilized with increasing mesh density. When the mesh size was reduced from 1.0 mm to 0.8 mm, the resulting change in maximum deformation was within 3%. Therefore, to balance computational cost and solution precision, a mesh size of 1.0 mm was selected for subsequent finite element analyses.

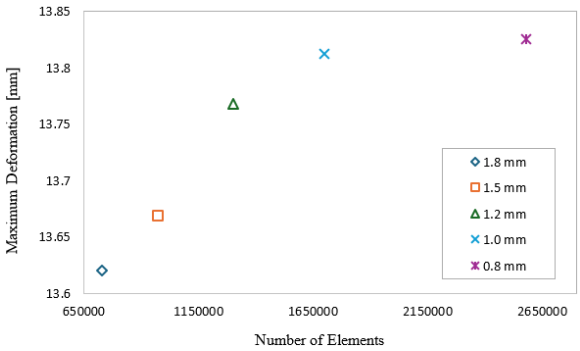

Figure 5. Mesh convergence analysis

Material Effects in Bicycle Frame Impact Test

To evaluate the feasibility of applying natural fiber-reinforced composites to bicycle frame structures, this study selected sisal and jute as natural reinforcement fibers. An impact test simulation was conducted based on the ISO 4210-6 standard to investigate the differences in impact response of the frame structure using the two materials. To improve

computational efficiency, this study defined a composite stacking block composed of four laminae with fiber orientations of 0°, 30°, 60°, and 90°, which served as the basic lay-up configuration for modeling the bicycle front fork. The analysis further aimed to determine the minimum number of layers required to satisfy the structural criteria of the impact test under various global ply orientation combinations.

Figures 6 and 7 illustrate that, for both sisal and jute fiber-reinforced composites, the maximum deformation decreases with an increasing number of stacking blocks under various ply orientations. When the lay-up reaches seven stacking blocks (i.e., 28 individual laminae, totaling 5.6 mm in thickness), the maximum deformation for both materials under 0° and 90° global ply orientations falls below the 10 mm compliance threshold specified in ISO 4210-6. Specifically, at the 0° orientation, the maximum deformation values were 7.7361 mm for sisal and 8.676 mm for jute, while at the 90° orientation, they were 8.4683 mm and 9.057 mm, respectively. These results indicate that, at the same total laminate thickness, the stiffness of the sisal fiber composite is higher than that of the jute fiber composite. Figures 8 (a)-(b) show the deformation distributions of the sisal and jute composites under global orientations of 0° and 90°, respectively.

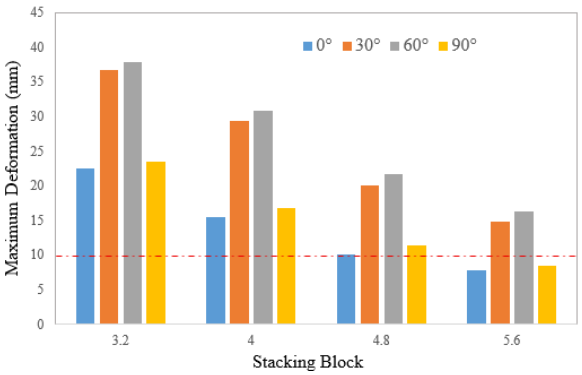

Figure 6. Maximum Deformation versus Stacking Block under Various Ply Orientations (Sisal)

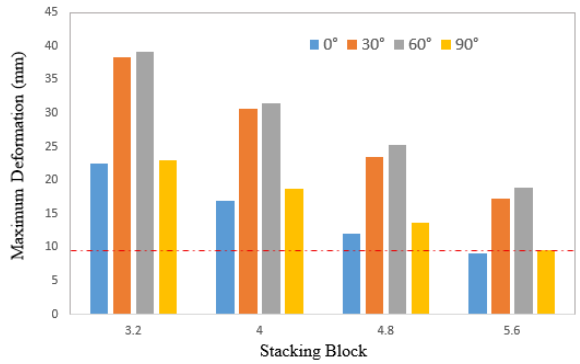

Figure 7. Maximum Deformation versus Stacking Block under Various Ply Orientations (jute)

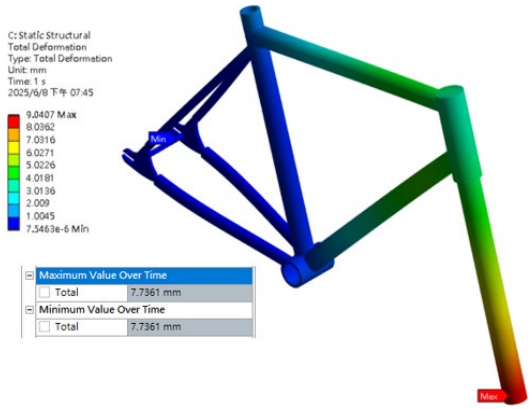

(a)

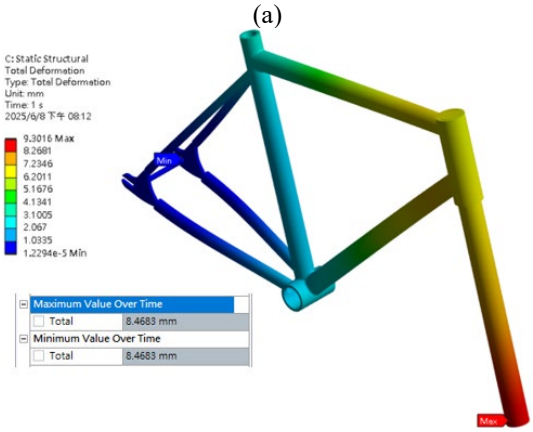

(b)

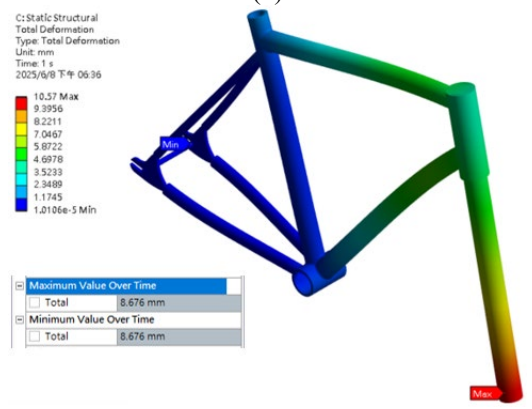

(c)

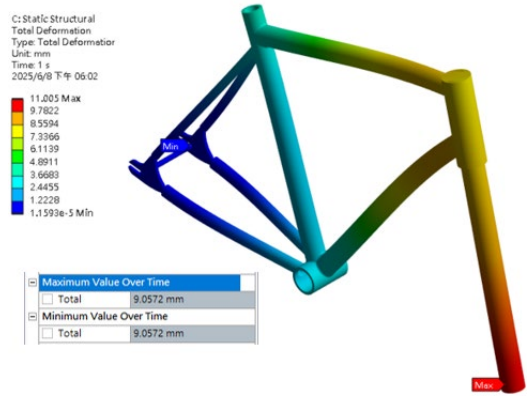

(d)

Figure 8. Deformation Distributions of Sisal and Jute Composites under 0° and 90° Orientations: (a) Sisal at 0°, (b) Jute at 0°, (c) Sisal at 90°, (d) Jute at 90°

Reinforcement Strategies for Impact Performance Improvement

To achieve a lightweight design and reduce the overall weight of the bicycle frame, this study evaluates the feasibility of localized reinforcement. Considering the condition where the structure does not yet satisfy the ISO 4210-6 impact test requirement (i.e., fewer than seven stacking blocks), it is known that the maximum deformation primarily occurs in the top tube and down tube regions. Without accounting for the front fork component, these two areas were selected as reinforcement zones to further investigate the effectiveness of local reinforcement in improving the overall deformation performance of the bicycle frame.

Based on the results shown in Figures 9 and 10, the reinforcement effectiveness of sisal and jute fiber-reinforced composite bicycle frames was evaluated under the condition of local reinforcement applied to the top tube. Figure 9 illustrates the maximum deformation of the sisal fiber composite at the top tube under different ply orientations. For ply orientations of 0° and 30°, the local reinforcement was sufficient to reduce the maximum deformation to 9.5059 mm and 9.9833 mm, respectively. However, for orientations of 60° and 90°, the corresponding deformation values were 10.144 mm and 10.15 mm, indicating that the reinforcement was insufficient to satisfy the standard.

Figure 10 illustrates the maximum deformation of the jute fiber composite at the top tube under different ply orientations. Compared to sisal, the jute composite required a greater reinforcement thickness to meet the compliance standard. Only the 0° ply orientation achieved the required performance, where a three-layer local reinforcement (0.6 mm) reduced the deformation to 9.8959 mm. For the 30°, 60°, and 90° orientations, the deformation values remained above the 10 mm threshold, at 11.034 mm, 11.674 mm, and 11.698 mm, respectively. These results indicate that, under identical local reinforcement conditions, the sisal composite offered superior structural stiffness compared to jute.

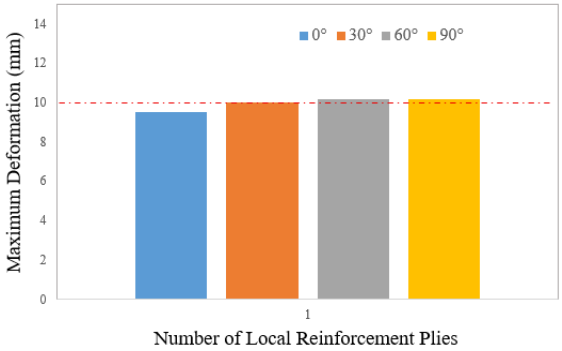

Figure 9. Maximum Deformation under Different Ply Angles with Local Reinforcement on the Top Tube (Sisal)

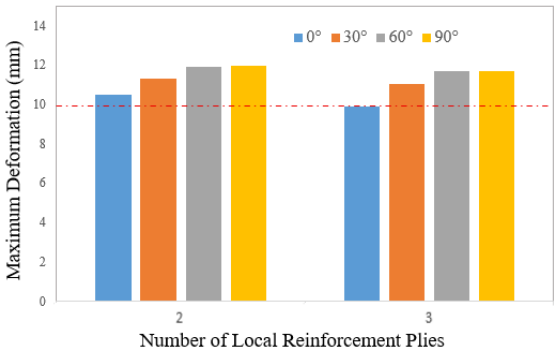

Figure 10. Maximum Deformation under Different Ply Angles with Local Reinforcement on the Top Tube (Jute)

Figures 11 and 12 present the analysis of local reinforcement applied to the down tube region for bicycle frames made from sisal and jute fiber-reinforced composites. The deformation results under various ply orientations were compared to assess the structural improvement achievable through localized reinforcement in this area. As shown in Figure 11, when a single-layer local reinforcement was applied to the down tube region, the sisal fiber-reinforced composite frame exhibited maximum deformations of 9.5256 mm and 9.9555 mm under ply orientations of 0° and 30°, respectively—both satisfying the ISO 4210-6 compliance limit of 10 mm with just one additional layer. However, for orientations of 60° and 90°, the maximum deformations reached 10.147 mm and 10.15 mm, indicating non-compliance with the standard.

In comparison, the jute fiber-reinforced composite frame required a greater reinforcement thickness to satisfy the criterion. As shown in Figure 12, only the 0° ply orientation met the requirement when three additional layers (0.6 mm) were applied, reducing the deformation to 9.9982 mm. Under the same reinforcement conditions, the deformation values for the 30°, 60°, and 90° orientations were 11.025 mm, 11.681 mm, and 11.587 mm, respectively—each exceeding the 10 mm threshold.

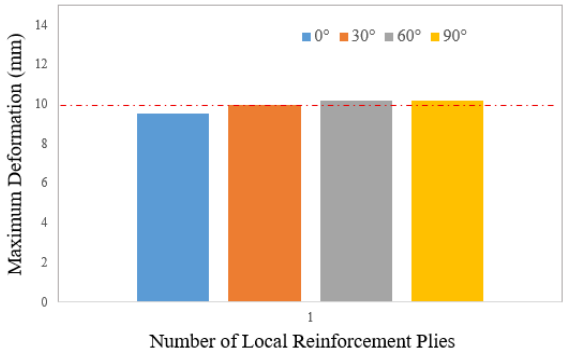

Figure 11. Maximum Deformation under Different Ply Angles with Local Reinforcement on the Down Tube (Sisal)

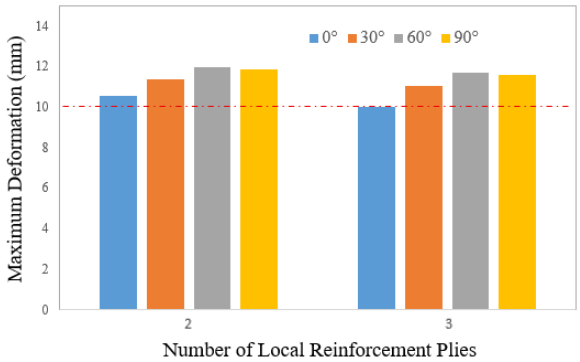

Figure 12. Maximum Deformation under Different Ply Angles with Local Reinforcement on the Down Tube (Jute)

Finally, after confirming the superior reinforcement effectiveness of sisal over jute, a comparative evaluation was conducted between local reinforcements applied to the top and down tubes. The maximum deformation after reinforcing the top tube was 9.5059 mm, while that of the down tube was 9.5256 mm. These results indicate that the top tube exhibited a more pronounced reinforcement effect, demonstrating better deformation suppression efficiency.

CONCLUSIONS

This study employed finite element analysis (FEA) to evaluate the feasibility of applying natural fiber-reinforced composites to bicycle frame structures, using the ISO 4210-6 impact test standard as the simulation benchmark. Sisal and jute were selected as natural reinforcement fibers, combined with epoxy resin as the matrix material, to construct various bicycle frame models with different ply orientations and stacking configurations. The key findings are as follows:

1. Under identical thickness and stacking conditions, the sisal fiber composite exhibited superior structural stiffness and impact resistance compared to the jute fiber composite.
2. For the full-frame configuration using sisal fiber-reinforced composites, a total of 28 layers was required to pass the ISO 4210-6 impact test.
3. Among the local reinforcement strategies, reinforcing the top tube led to a greater reduction in deformation than the down tube, showing that reinforcement was more effective in the top tube area.
4. Overall, sisal fibers demonstrated greater potential for structural reinforcement applications. Through the development of simulation models and numerical analysis, this study provides theoretical support for the feasibility of applying natural fiber-reinforced composites to bicycle frame structures, serving as a reference for future physical manufacturing and design development.

Acknowledgments

The continuous financial support from the National Science and Technology Council in Taiwan is greatly acknowledged.

REFERENCES

Chaikittiratana, A., Suwanpakpraek, K., Pornpeerakeat, S., Limrungruengrat, S., & Dietz-Röthlingshöfer, J., “Bicycle frame from hemp fibre filament wound composites,” *Technologies for Lightweight Structures*, 3(1), 42–49 (2019).

Fao, H. R., Jasron, J. U., Bunganaen, W., & Boimau, K., “Pengaruh perlakuan temperatur terhadap sifat mekanik komposit hibrid polyester berpenguat serat buah lontar dan serat kaca,” LONTAR Jurnal Teknik Mesin Undana, 3(1), 27-36 (2016).

International Organization for Standardization., *ISO 4210-6: Cycles – Safety requirements for bicycles – Part 6: Wheels and rims*. ISO (2014).

Khan, F., Hossain, N., Hasan, F., Rahman, S. M. M., Khan, S., Saifullah, A. Z. A., & Chowdhury, M. A., “Advances of natural fiber composites in diverse engineering applications—A review,” *Applications in Engineering Science*, 18, 100184 (2024).

Karimah, A., Ridho, M. R., Munawar, S. S., Adi, D. S. W., Ismadi, I., Damayanti, R., Subiyanto, B., Fatriasari, W., & Fudholi, A., “A review on natural fibers for development of eco-friendly bio-composite: Characteristics, and utilizations,” *Journal of Materials Research and Technology*, 13, 2442–2458 (2021).

Khalid, M. Y., Al Rashid, A., Arif, Z. U., Ahmed, W., Arshad, H., & Zaidi, A. A., “Natural fiber reinforced composites: Sustainable materials for emerging applications,” *Results in Engineering*, 11, 100263 (2021).

Lin, C.-C., Huang, S.-J., & Liu, C.-C., “Structural analysis and optimization of bicycle frame designs,” *Advances in Mechanical Engineering*, 9(12), 1–10 (2017).

Naveen, P. N. E., & Reddy, R. B., “An analysis of composite drive shaft using ANSYS ACP,” *International Journal of Mechanical and Production Engineering Research and Development*, 8(5), 117–124 (2018).

Nurazzi, N. M., Asyraf, M. R. M., Fatimah Athiyah, S., Shazleen, S. S., Rafiqah, S. A., Harussani, M. M., Kamarudin, S. H., Razman, M. R., Rahmah, M., Zainudin, E. S., Ilyas, R. A.,

Aisyah, H. A., Norrrahim, M. N. F., Abdullah, N., Sapuan, S. M., & Khalina, A., "A review on mechanical performance of hybrid natural fiber polymer composites for structural applications," *Polymers*, 13(13), 2170 (2021).

Rahman, M. Z., "Mechanical and damping performances of flax fibre composites – A review," *Composites Part C: Open Access*, 4, 100081 (2021).

Saravanan, K. G., Prabu, R., Sivapragasam, A., & Daniel, N., "Comparative analysis of natural fibre reinforced composite material using ANSYS," *Advances in Materials Science and Engineering* 2021(1) 9391237 (2021).

SolidWorks, Composite Shells—Ply Angle Definition, SolidWorks, (2025).